Cell PRESS
Open ACCESS

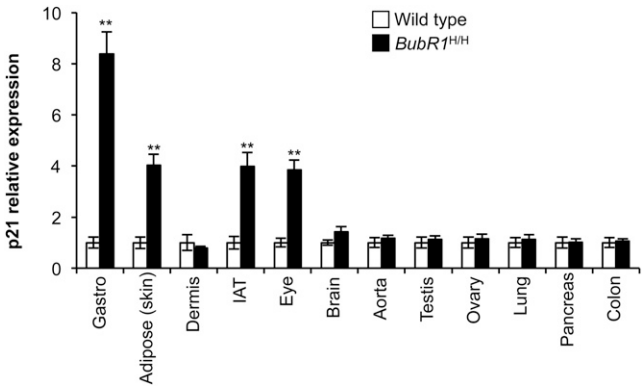

Figure S1. *p21* Is Induced in Select Prematurely Aged *BubR1*$^{H/H}$ Tissues, Related to Figures 1 and 2

qRT-PCR analysis of various tissues from 2-month-old mice analyzed for *p21* expression. Data are mean ± s.d. (n = 5 mice of each genotype). Asterisks denote significant differences compared to wild-type mice. **$p < 0.01$. See also Figures 1 and 2.

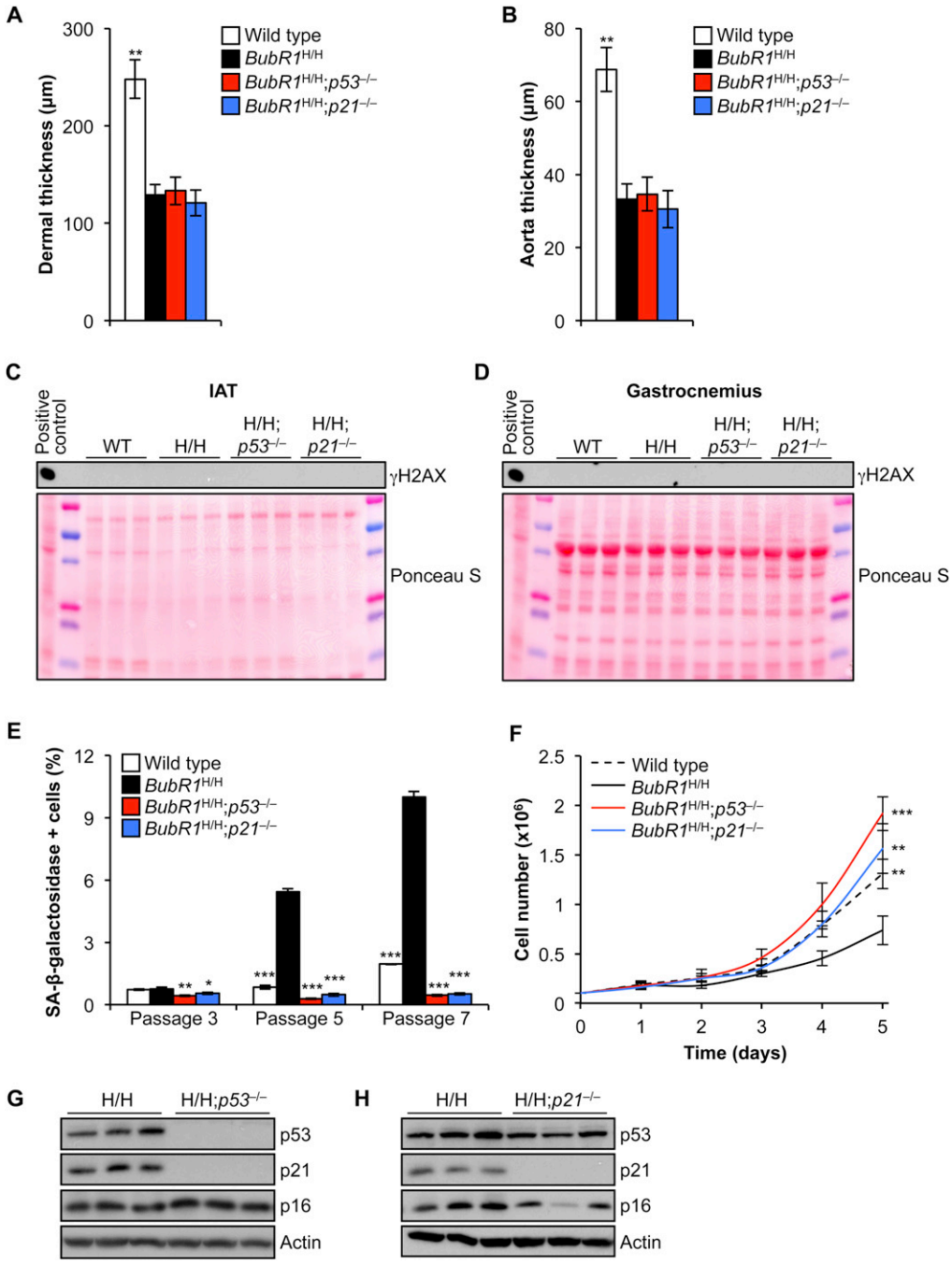

Figure S2. Growth and DNA Damage Rates of *BubR1*$^{H/H}$ MEFs Lacking *p53* or *p21*, Related to Figures 2 and 3

(A and B) Dermal (A) and aorta (B) thickness in 2-month-old mice. Data are mean ± s.d. (n = 5 mice of each genotype). Asterisks denote significant differences compared to *BubR1*$^{H/H}$ mice, **p < 0.01.

(C and D) DNA damage, as assessed by γH2AX Western blotting, is not detected in IAT (C) or skeletal muscle (D) extracts of 2-month-old mice. Ponceau S staining was used to equalize loading.

(E) SA-β-gal positive cells in passage 3, 5 and 7 MEF cultures.

(F) In vitro growth curves of passage 7 MEF cultures of the indicated genotypes. For each genotype and passage in (E) and (F), three independent MEF lines were used. Values represent mean ± s.d. Asterisks denote significant differences compared to *BubR1*$^{H/H}$ mice, **p < 0.01, ***p < 0.001.

(G and H) Western blot of passage 7 *BubR1*$^{H/H}$ and *BubR1*$^{H/H}$;*p53*$^{-/-}$ (G) and *BubR1*$^{H/H}$ and *BubR1*$^{H/H}$;*p21*$^{-/-}$ (H) MEF extracts probed with p16^{Ink4a}, p19^{Arf}, p21 and p53 antibodies. Actin was used as a loading control.

See also Figures 2 and 3.

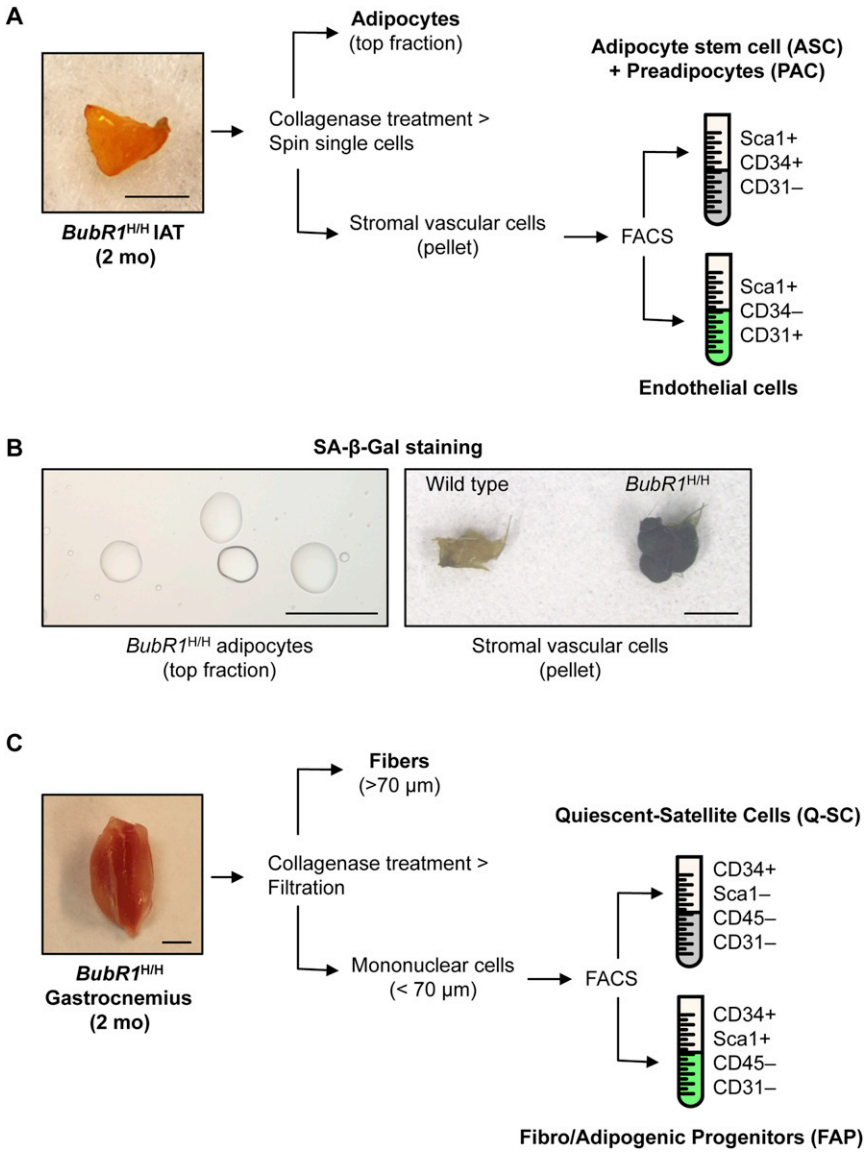

Figure S3. Schematic Overview of Experimental Approaches Used to Identify Senescent Cell Types in Skeletal Muscle and Fat, Related to Figures 4 and 5

(A) IAT of 2-month-old *BubR1*$^{H/H}$ mice was first collagenase treated and separated into the mature adipocytes and the SVF by centrifugation. Cells in the SVF were labeled with antibodies for Sca-1, CD34 and CD31 and FACS sorted into ASC/PAC and endothelial cell subpopulations. Scale bar, 5 mm.

(B) SA-β-gal staining on indicated fractions prepared in (A). Scale bars, 100 μm (left) and 1 mm (right).

(C) Schematic for isolation of fibers, Q-SCs, Ac-SCs and FAPs from gastrocnemius muscle of 2-month-old *BubR1*$^{H/H}$ mice. Mononuclear cells obtained after collagenase digestion were stained with antibodies for Sca-1, CD31, CD34 and CD45. Scale bar, 1 mm.

See also Figures 4 and 5.

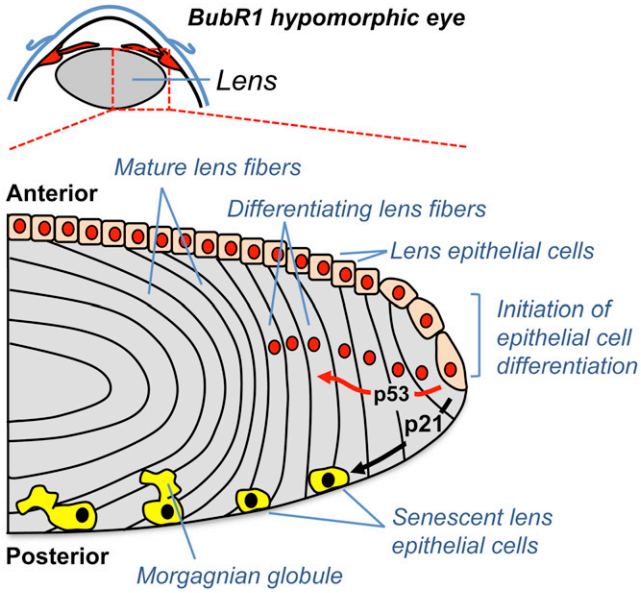

Figure S4. Model for Posterior Subcapsular Cataract Formation in BubR1 Progeroid Mice, Related to Figure 6

Epithelial cells positioned in the equator initiate a terminal differentiation into elongated mature lens fibers. This process is impaired in BubR1 progeroid mice, resulting in accumulation of aberrantly differentiated epithelial cells at the posterior part of the lens, where they form Morgagnian globules and disrupt the normal architecture of the lens and promote cataract formations. Accumulation of epithelial cells with senescent properties and cataract formation are markedly reduced in BubR1 progeroid mice lacking p21, suggesting that this p53 target drives these pathogenic events. Inactivation of p53 has the converse effect, suggesting that p53 acts to prevent mislocalization and senescence of lens epithelial cells though a p21-independent mechanism. See also Figure 6.